Pergamon

SCIENCE DIRECT®

Tetrahedron Letters 44 (2003) 7299–7302

TETRAHEDRON LETTERS

# The cation-π cloud interaction and the zeolite basicity concept☆

Rodrigo J. Corrêa*

*Instituto de Química, Departamento de Química Orgânica, Universidade Federal do Rio de Janeiro, Cidade Universitária, CT Bloco A, Ilha do Fundão, Rio de Janeiro/RJ, Brazil, 21949-900*

Received 27 June 2003; revised 31 July 2003; accepted 1 August 2003

**Abstract**—Two adsorption complexes between pyrrole and alkaline $T_6$ zeolite clusters were studied theoretically using DFT method. Results show that at B3LYP/6-311+G**//B3LYP/6-31G* the oxygen atoms in $LiT_6$ are, in average, more charged than in $CsT_6$. The cation-π complex is more stable than the complex possessing a hydrogen bond between $T_6$ clusters and pyrrole. Correlations between alkaline cation hardness and $\Delta H_{adsorption}$ (kcal/mol) showed a linear correlation for both complexes, indicating that the driving force for pyrrole adsorption is cation hardness.


Zeolites are aluminosilicates with a tridimensional structure that form channels and cages of molecular dimensions. The aluminum atoms in the zeolite framework are tetracoordinated, hence developing a negative charge on the structure, which is compensated by extraframework cations of different charges. Ion exchange techniques are usually employed for changing the cationic species and can be used to yield acid or basic zeolites, depending on the nature of the counter ion: zeolites with protons and metal ions generate acid or basic sites, respectively.[1,2]

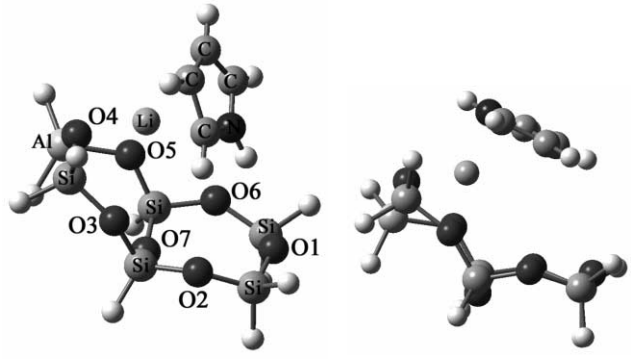


**Figure 1.** Pyrrole adsorption modes on $MT_6$.

Zeolites can be used to accomodate organic molecules since their properties can be varied in host–guest systems. The importance of cation-π interactions has been thoroughly documented for biological systems[3–8] and it is now believed that it might also be an important factor in controlling the properties of the organic probe molecules inside zeolites. This proposal is sustained by results showing that the photophysical behavior of organic chromophores are directly related to the counter ions nature and the presence of adsorbed water.[9]

In solid materials it is believed that basicity is due to the charge on the oxygen atoms, which in turn is either related to the cation eletropositivity or to the Si/Al ratio. Attempts to correlate basicity with structural zeolite parameters using both computational and experimental methodologies have been carried out with probe molecules such as pyrrole (N–H stretching vibration),[10–12] methanol (OH stretching vibration),[13,14] methyl viologen and $I_2$ (charge transfer in UV–vis),[15,16] chlorocarbon adsorption ($^1$H NMR)[17–20] and CO and $CO_2$ adsorption.[21–24] Regardless of the differences in probes and methodologies, the quantity measured correlates in all cases quite well with the zeolite oxygen charges, obtained by applying Sanderson's equalization principle.

Theoretical methods based on quantum mechanics (DFT) have been employed to investigate the concept of basic centers in solid materials.[25–27] Results show that the Mulliken oxygen charge does not change significantly from the $Na^+$ to $Cs^+$ counter ion.[28] This means that Sanderson's principle should not be an adequate tool for estimating the zeolite oxygen charges.

☆ Supplementary data associated with this article can be found at doi:10.1016/S0040-4039(03)01880-X

* Tel.: +51-21-2562-7363; fax: +51-21-2562-7256; e-mail: rcorrea@iq.ufrj.br

0040-4039/$ - see front matter © 2003 Elsevier Ltd. All rights reserved.
doi:10.1016/S0040-4039(03)01880-X

Furthermore, one cannot expect the equalization principle to reproduce molecular complexity since it cannot accommodate differences associated with isomerism.

The present study evaluated charges and energetic profiles for pyrrole adsorption on the alkaline metal–$T_6$ ($MT_6$, SIII site) clusters, in order to clarify the main aspects concerning the adsorption of organic probes on zeolites. The framework of alkaline metal–$T_6$ ($MT_6$) was taken from a complete faujasite cage, manually constructed based on X-ray diffraction results.

The structure geometries were fully optimized (Fig. 1) and they were characterized by the absence of imaginary frequencies, after vibrational analysis on the optimized geometries. Calculations of free and adsorbed reactants, as well their respective charges, were performed at B3LYP/6-311+G**//B3LYP/6-31G* and with Lanl2dz for K, Rb and Cs level methodology. Zero-point and thermal corrections at 298 K were calculated utilizing the frequencies computed at the B3LYP/6-31G*. In all structures charges at the atomic centers were calculated by fitting to the density derived electrostatic potential with the CHelpG scheme.[28] All calculations were performed using the GAUSSIAN 94 package.[29] The level of theory employed here has been proved to be adequate in determining both zeolite geometric parameters, and activation barriers for reactions within zeolite cages and the energetics associated with cation-π interactions.[30,31]

## Results and discussion

Calculations show that pyrrole adsorbs on alkaline metals $MT_6$ cluster by two different modes (Fig. 1). The first mode involves a complex with a hydrogen bond being formed between the probe molecule and the zeolite cluster (Mode 1), whereas the second one shows only the interaction between the pyrrole π cloud and the alkaline metals (Mode 2).

From the $O_4$–M distances on $MT_6$ shown in Table 1, two slightly different cation sites related to Site III can be observed. While Li–$O_4$ is 1.945 Å apart, we find a value of 3.241 Å for Cs–$O_4$. The results show that $Na^+$, $Li^+$ and $K^+$ are closer to oxygens $O_4$ and $O_5$ (almost symmetrically), while $Rb^+$ and $Cs^+$ are located above $O_7$ and closer to $O_6$, in the middle of SIII site.

In Mode 1, the NH distances are relatively constant, varying by only 0.002 Å (Table 1), while for Mode 2 a 0.006 Å variation can be seen. This means that NH bond in the pyrrole molecule is not sensitive to zeolite charge. Observing the angle $\phi$ (not shown in Table 1) formed between the pyrrole plane and the counter ions, it can be seen that for $Rb^+$ and $Cs^+$ this angle reaches 90°, which is probably due to a drastic reduction of the cation's hardness. The M–Al distances can also evidence the strong interaction between metal cations and pyrrole π cloud. In Mode 1 the M–Al distances are increased by an average of 0.07 Å. Notwithstanding, these elongations are more evident when going from $MT_6$ to Mode 2, where we find an average of 0.15 Å increase. These results show that a non-hydrogen bonded adsorption mode for pyrrole on $MT_6$ (Mode 2) causes cations to be pushed away from the zeolite framework.

Table 1 shows the energy profiles for the pyrrole adsorption modes. It can be seen that in Mode 1 the strongest interaction is obtained with $LiT_6$ (−12.8 kcal/mol) and it decreases continuously, reaching a minimum with $Cs^+$ (−7.2 kcal/mol). In Mode 2, only pyrrole adsorption on $LiT_6$ is less stable than Mode 1, varying by 0.4 kcal/mol (where $O_1$ is the least charged). From $NaT_6$ to $CsT_6$, Mode 2 is the most stable structure. This trend shows that, although $O_1$ in $CsT_6$ has a more pronounced charge than the other oxygen atoms in the framework, this is not necessarily the driving force for adsorption. In pyrrole–$MT_6$, the most important interaction is a cation-π cloud.

It is interesting to note the binding energy magnitudes in Table 1. As can be seen, both modes are, as expected, much less exothermic than vapor phase calculations for aromatics compounds.[32,33] In this sense, it is clear that alkaline cations are quite well coordinated in zeolite SIII site. Thus, in this study, the cation-π interaction can be assigned as a kind of intermolecular interaction, rather than a chemical bonding.

**Table 1.** Geometric and energetic parameters for pyrrole adsorption on $MT_6$

| | $MT_6$ | | | Mode 1 | | | | | Mode 2 | | | | |
|---|---|---|---|---|---|---|---|---|---|---|---|---|---|
| Cation | Al–M[a] | O4–M[a] | O7–M[a] | Al–M[a] | O4–M[a] | N–H[a] | M–Pyrrole[b] | B.E.[c] | Al–M[a] | M–Pyrrole[b] | O4–M[a] | N–H[a] | B.E.[c] |
| Li | 2.632 | 1.945 | 3.142 | 2.648 | 1.945 | 1.019 | 2.131 | −12.8 | 2.714 | 2.155 | 2.115 | 1.015 | −12.4 |
| Na | 2.719 | 2.338 | 3.691 | 2.958 | 2.339 | 1.018 | 2.512 | −9.0 | 3.016 | 2.524 | 2.351 | 1.019 | −12.3 |
| K | 3.118 | 2.795 | 4.061 | 3.165 | 2.802 | 1.017 | 2.952 | −8.1 | 3.477 | 2.927 | 2.750 | 1.018 | −8.7 |
| Rb | 3.344 | 3.001 | 4.290 | 3.378 | 3.071 | 1.017 | 3.231 | −7.5 | 3.646 | 3.191 | 3.061 | 1.022 | −9.1 |
| Cs | 3.573 | 3.244 | 4.475 | 3.590 | 3.241 | 1.017 | 3.491 | −7.2 | 3.866 | 3.449 | 3.312 | 1.023 | −8.7 |

[a] Distances in Å.
[b] Distances metal–pyrrole in Å.
[c] Binding energies in kcal/mol.

The computed N–H frequencies from Modes 1 and 2 are in opposite directions. In Mode 1 there is a frequency increase from Li to Cs (Li = 3325, Na = 3341, K = 3353, Rb = 3361 and Cs = 3354 $cm^{-1}$), while in Mode 2 an opposite trend is found (Li = 3404, Na = 3334, K = 3358, Rb = 3270 and Cs = 3255 $cm^{-1}$). In fact, the Mode 2 trend corresponds with the experimentally observed for Y zeolites (LiY = 3435, NaY = 3390, KY = 3320, RbY = 3280 and CsY = 3240 $cm^{-1}$).[16] Moreover, O1 charges increase in the inverse direction to the Mode 2 NH frequencies, once again as expected from the experimental results.

Table 1 also shows the metal–pyrrole distances in Mode 1 and Mode 2 (M–pyrrole). As can be seen, in both cases this parameter enhances from $Li^+$ to $Cs^+$, and for the same counter ion these values are quite similar. This indicates that regardless of hydrogen bond in Mode 1, the driving force between the probe and the zeolite cluster is the cation-π interaction.

The oxygen atoms $O_3$, $O_4$, $O_5$ and $O_7$, generally possess the highest charges in the alkaline series ($LiT_6$, $O_5$, $q = -0.905e$), decreasing continuously from Li to Cs ($CsT_6$, $O_5$, $q = -0.822e$) (Table 2, supplementary material). It is interesting to note that these oxygen atoms are closest to the metal cations $Li^+$, $Na^+$ and $K^+$. The atoms $O_1$, $O_2$ and $O_6$ are the least charged on $MT_6$ clusters (and farthest from $Li^+$, $Na^+$ and $K^+$), creating a charge gradient in the zeolite framework. As the distance $O_1$–M diminishes from Li to Cs, the charges on $O_1$, $O_2$ and $O_6$ increase continuously, suggesting that the closer the oxygen atom is to the metal cation, the higher its charge will be (this effect is evident for $qO_5 \gg qO_6 > qO_2 > qO_1$). Examining the charges in $O_4$ and $O_5$ one can see that in both adsorption modes the absolute values decreases, although the reduction is more evident in Mode 2. Also from Table 1 we also note that Mode 2 is responsible for a greater increase of M–Al distances, caused by a preferential interaction between the cations and the pyrrole molecule. These results indicate that Mode 2 better illustrates charge transfer in alkaline metal cation than Mode 1. This statement can also be confirmed by observing that, in Mode 2, the counter ions possess lower positive charge due to a better interaction with the organic probe (Table 2, supplementary material).

All computed values correlate quite well with the nature of the cation. In fact, a good correlation between computed cation hardness (from cation charge/volume ratios) and Mode 1 heat of adsorption ($\Delta H°$) was found with $r^2 = 0.988$. Other good correlations were also found: Plotting Mode 1 heat of adsorption ($\Delta H°$) and NH Mode 1 stretching frequencies, gives $r^2 = 0.918$, and by a linear plot with O1 ab initio computed charge and cation hardness, an $r^2 = 0.994$ correlation was obtained. Moreover, correlating O1 charges with NH Mode 1 stretching frequencies, gives an $r^2 = 0.927$ correlation. Other good correlations can also be obtained with Mode 2. Thus, since O1 charges correlates with NH frequencies and cation hardness, it follows that cation hardness correlates with NH frequencies. In fact, this indicates that such measurements are cross correlations. It is important to address here that, for Mode 2, both heat of adsorption ($\Delta H°$) and NH frequencies have negative slopes when plotted with O1 charges, but for Mode 1, the slopes have opposite signs. Such results indicate that experimental measurements are obtained when a cation-π interaction like Mode 2 is the most important binding mode.

The results presented here show that the most stable pyrrole adsorption structure is controlled by a cation-π type interaction, instead of being governed by oxygen charges (regardless of it being computed by Sanderson's equalization principle).

## Acknowledgements

The author thanks Professor D. E. Nicodem, P. M. Esteves, Dr. L. M. Estevão for the valuable discussions and Dept. Biofísica of UFRJ for computational support.

## References

1. Murray, D. K.; Chang, J. W.; Haw, J. F. *J. Am. Chem. Soc.* **1993**, *115*, 4732–4741.
2. Gorte, R. J. *Catal. Lett.* **1999**, *62*, 1–13.
3. Dougherty, D. A. *Science* **1996**, *271*, 163–168.
4. (a) Dougherty, D. A.; Stauffer, D. A. *Chem. Rev.* **1997**, *97*, 1303; (b) Sussman, J. L.; Harel, M.; Frolow, F.; Oefner, C.; Goldman, A.; Tolker, L.; Silman, I. *Science* **1991**, *253*, 872–879.
5. Tsuzuki, S.; Yoshida, M.; Uchimaru, T.; Mikami, M. *J. Phys. Chem. A.* **2001**, *105*, 769–773.
6. Komori, Y.; Hayashi, S. *Langmuir* **2003**, *19*, 1987–1989.
7. Busch, D. H. *Chem. Rev.* **1993**, *93*, 847–860.
8. Kim, K. S.; Tarakeswar, P.; Lee, J. Y. *Chem. Rev.* **2000**, *100*, 4145–4185.
9. Thomas, K. J.; Sunoj, R. B.; Chandrasekhar, J.; Ramamurthy, V. *Langmuir* **2000**, *16*, 4912–4921.
10. Sánchez-Sánchez, M.; Blasco, T. *Chem. Commun.* **2000**, 491–492.
11. Murphy, D.; Massiani, P.; Franck, R.; Barthomeuf, D. *J. Phys. Chem.* **1996**, *100*, 6731–6738.
12. Huang, M.; Kaliaguine, S. *J. Chem. Soc., Faraday Trans.* **1992**, *88*, 751–758.
13. Rep, M.; Palomares, A. E.; Eder-Mirth, G.; van Ommen, J. G.; Rösc, N.; Lercher, J. A. *J. Phys. Chem. B* **2000**, *104*, 8624–8630.
14. Kogelbauer, A.; Grûndling, C.; Lercher, J. A. *J. Phys. Chem.* **1996**, *100*, 1852–1857.
15. Choi, S. Y.; Park, Y. S.; Hong, S. B.; Yoon, K. B. *J. Am. Chem. Soc.* **1996**, *118*, 9377–9386.
16. Ranjit, K. T.; Kevan, L. *J. Phys. Chem. B* **2002**, *160*, 1104–1109.
17. Sánchez-Sánchez, M.; Blasco, T.; Rey, F. *Phys. Chem. Chem. Phys.* **1999**, *1*, 4529–4535.
18. Bosh, E.; Huber, S.; Weitkamp, J.; Knözinger, H. *Phys. Chem. Chem. Phys.* **1999**, *1*, 579–584.

19. Timonen, J. T.; Pakkanen, T. T. *Micropor. Mesopor. Mater.* **1999**, *1*, 327–333.
20. Mellot, C. F.; Cheetham, A. K.; Harmis, S.; Savitz, S.; Gorte, R. J.; Myers, A. L. *J. Am. Chem. Soc.* **1998**, *120*, 5788–5792.
21. Ferrari, A. M.; Neyman, K. M.; Rösch, N. *J. Phys. Chem. B* **1997**, *101*, 9292–9298.
22. Laspéras, M.; Cambon, H.; Brunel, D.; Rodriguez, I.; Geneste, P. *Micropor. Mater.* **1993**, *1*, 343–351.
23. Okamoto, Y.; Kubota, T. *Micropor. Mesopor. Mater.* **2001**, *48*, 301–307.
24. Bonelli, B.; Civalleri, B.; Fubini, B.; Ugliengo, P.; Areán, C. O.; Garrone, E. *J. Phys. Chem. B* **2000**, *104*, 10978–10988.
25. Deka, R. Ch.; Roy, R. K.; Hirao, K. *Chem. Phys. Lett.* **2000**, *332*, 576–582.
26. Vayssilov, G. N.; Lercher, J. A.; Rösch, N. *J. Phys. Chem. B* **2000**, *104*, 8614–8623.
27. Sponer, J. E.; Sobalík, Z.; Leszczynski, J.; Wichterlóva, B. *J. Phys. Chem. B* **2002**, *105*, 8285–8290.
28. (a) Chirlian, L. E.; Francl, M. M. *J. Comput. Chem.* **1997**, *8*, 894; (b) Breneman, C. M.; Wiberg, K. B. *J. Comput. Chem.* **1991**, *11*, 361.
29. M. J. Frisch, G. W. Trucks, H. B. Schlegel, G. E. Scuseria, M. A. Robb, J. R. Cheeseman, V. G. Zakrzewski, J. A. Montgomery Jr., R. E. Stratmann, J. C. Burant, S. Dapprich, J. M. Millam, A. D. Daniels, K. N. Kudin, M. C. Strain, Ö. Farkas, J. Tomasi, V. Barone, M. Cossi, R. Cammi, B. Mennucci, C. Pomelli, C. Adamo, S. Clifford, J. Ochterski, G. A. Petersson, P. Y. Ayala, Q. Cui, K. Morokuma, P. Salvador, J. J. Dannenberg, D. K. Malick, A. D. Rabuck, K. Raghavachari, J. B. Foresman, J. Cioslowski, J. V. Ortiz, A. G. Baboul, B. B. Stefanov, G. Liu, A. Liashenko, P. Piskorz, I. Komáromi, R. Gomperts, R. L. Martin, D. J. Fox, T. Keith, M. A. Al-Laham, C. Y. Peng, A. Nanayakkara, M. Challacombe, P. M. W. Gill, B. Johnson, W. Chen, M. W. Wong, J. L. Andres, C. Gonzalez, M. Head-Gordon, E. S. Replogle, and J. A. Pople, Gaussian 98 (Gaussian, Inc., Pittsburgh, PA, 1998).
30. Nicholas, J. B.; Hay, B. P. *J. Phys. Chem. B* **1999**, *103*, 9815–9820.
31. Nicholas, J. B.; Hay, B. P.; Dixon, D. A. *J. Phys. Chem. A* **1999**, *103*, 1394–1400.
32. Zhu, W.; Tao, X.; Shen, J.; Luo, X.; Cheng, F.; Mok, P. C.; Ji, R.; Chen, K.; Jiang, H. *J. Phys. Chem. A* **2003**, *107*, 2296–2303.
33. Cheng, Y. H.; Liu, L.; Fu, Y.; Chen, R.; Li, X.; Guo, Q. *J. Phys. Chem. A* **2002**, *106*, 11215–11220.